

# Chest X-ray scanning based detection of COVID-19 using deepconvolutional neural network

Samir Yadav (✉ [ssyadav@dbatu.ac.in](mailto:ssyadav@dbatu.ac.in))

Dr. Babasaheb Ambedkar Technological University, Lonere, Raigad, India

Jasminder Kaur Sandhu

Chitkara University Institute of Engineering and Technology, Punjab, India

Yadunath Pathak

Indian Institute of Information Technology, Bhopal, India

Shivajirao Jadhav

Dr. Babasaheb Ambedkar Technological University, Lonere, Raigad, India

---

## Research Article

**Keywords:** Coronavirus, COVID-19, Chest X-rays, CNN, Transfer learning, CT scan

**Posted Date:** August 14th, 2020

**DOI:** <https://doi.org/10.21203/rs.3.rs-58833/v1>

**License:** © ⓘ This work is licensed under a Creative Commons Attribution 4.0 International License.

[Read Full License](#)

---

## **Chest X-ray scanning based detection of COVID-19 using deep convolutional neural network**

**Samir Yadav<sup>1</sup> · Jasminder Kaur Sandhu<sup>2</sup> ·  
Yadunath Pathak<sup>3</sup> · Shivajirao Jadhav<sup>4</sup>**

**Abstract** Everyone's life on earth influenced by a global coronavirus outbreak COVID-19. Two regular practices, pathology tests, and Computer Tomography (CT) scan used to diagnose COVID-19. Pathology tests produce a considerable amount of false-positives & are time-consuming, whereas CT scans tests are costly and require expert advice. Hence, the main aim of this work is to develop a fast, accurate, and low-cost diagnostic system for detection of COVID-19 using inexpensive chest X-rays and the modern Deep Convolutional Neural Network(CNN) approach to assist medical professionals. In this study, two pre-trained CNN models (VGG16 and InceptionV3) are evaluated by several experiments using data augmentations. The analysis is based on 2905 images of chest X-rays with 219 confirmed positive COVID-19 and 1345 positive pneumonia cases taken from the open-source database consisting of patients suffering from the COVID-19 disease. Since a database consists of multiple types of diseases, multiclass classification for diagnosis of COVID-19 is used. The InceptionV3 model provides the highest classification accuracy (99.35% and 98.29%) for two binary classifications (normal vs. COVID-19 and COVID-19 vs. Pneumonia) compare to VGG16 model's accuracy (97.71% and 96.27%). Whereas, VGG16 provides highest accuracy (98.84%)for multiclass-classification(normal vs COVID-19 vs pneumonia) as compared to VGG16 model's accuracy(96.35%).

**Keywords** Coronavirus · COVID-19 · Chest X-rays · CNN · Transfer learning · CT scan

---

Corresponding author:

<sup>3</sup>Samir Yadav

Assistant Professor,

Department of Information Technology,

Dr. Babasaheb Ambedkar Technological University, Lonere.

Mob.: +91-9011757323

E-mail: ssyadav@dbatu.ac.in

## 1 Introduction

COVID-19 is an exceptionally infectious disease caused by extremely severe respiratory symptoms Coronavirus 2 [1]. The virus was initially founded in Wuhan city of China, in December 2019. Thereafter this disease has reached all over the world, influencing more than 235 nations [2, 3]. Due to this, the World Health Organization (WHO) has announced the ongoing pandemic of COVID-19, a Public Health Emergency of International Concern. This has made several countries abroad implement policies to impose lockdown to prevent the spread of the Coronavirus. It is essential to detect infected people for quarantine and treatment procedures as soon as possible [4]. Till 2nd August 2020, there are a total of 17.6 million confirmed cases, 680 000 deaths and over the past seven days, the pandemic has continued to accelerate with almost 1.8 million new cases and 40 thousand new deaths reported a daily average of 256 294 cases and 5675 deaths per day. It took only 4 days for the number of cases to increase from 16 million to 17 million instances in approximately 235 countries and territories across the globe [5] shown in figure 1.

The test of COVID-19 is a problematical situation for everyone, even in developed nations, since the diagnosis system and its test kits are very limited and also not available everywhere in the world [6]. Currently, many researchers and institutes are working on diagnosis of COVID-19 disease [7, 8, 9, 10]. There are several ways to diagnose COVID-19 positive patients at early stages considering their symptoms as well as with the assistance of pathology test, Computer Tomography (CT) scan [11, 9]. To investigate early symptoms of COVID-19 is not a useful diagnostic procedure since there are some cases where people have the symptoms but are still not COVID -19 infected as confirmed by the pathological test or CT scan. Though the pathological test is one of the useful ways of diagnosing COVID-19 cases. However, this test has some limitations as they can be carried out in pathological labs which are available in city centers only and demand time-consuming precisions. This can cause a problem as the positive patients cannot be isolated earlier, and they can infect more people through the crucial time of unrestricted movement [12, 13]. CT scan is also one of

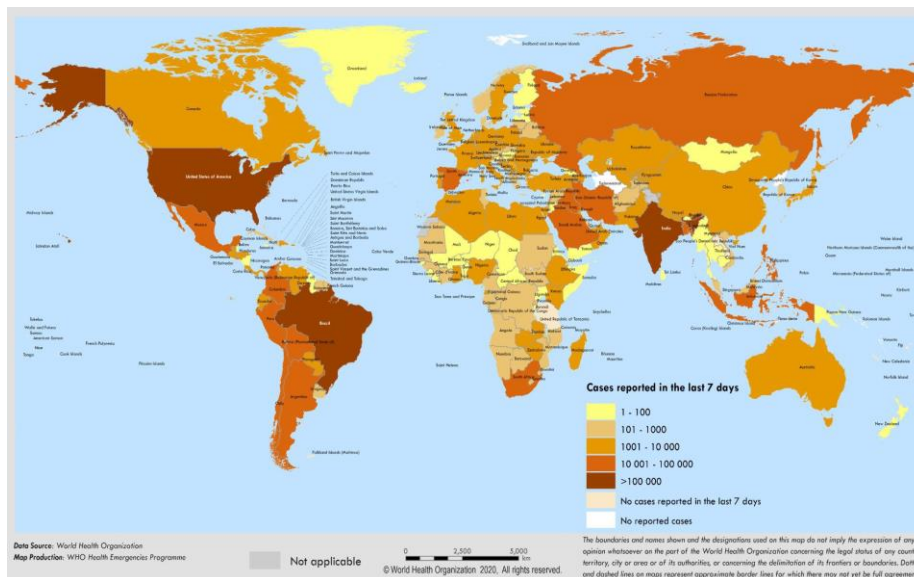


**Fig. 1** Total confirmed cases of COVID-19 by country and territory (as of 20 April 2020) [4]

the popular methods for diagnosis of COVID-19 [14]. However, the problem in this radiological imaging is the overlapping with other diseases. When a COVID-19 patient is infected with another lung disease such as pneumonia, then it is difficult for a medical professional or a radiologist to diagnose these both similar looking CT scan images [15]. Also, one of the major disadvantages of COVID-19 diagnosis using a CT scan is its high radiation dose and its high cost, as it is not easy for common people to use this procedure [16]. Traditional radiography or Chest X-Ray (CXR) images can overcome the problem of costly CT scans and pathological tests because CXR is less costly and has minimal harmful consequences. Also, CXR is capable of identifying various lung diseases earlier [17]. The CXR imaging is a non-invasive procedure that takes 2-3 minutes to capture the image, and results can be fetched within thirty minutes. The modern radiographical machines are affordable for average income countries or underdeveloped countries [18]. Hence, in this research work, CXR is used to identify the deadly COVID-19 coronavirus.

The X-rays are beneficial in diagnosing several diseases, on the other hand, the lack of medical professionals and radiologists for reviewing X-rays is a significant challenge all over the world. To review X-ray is a challenging task for an inexperienced radiologist be-

cause it does not contain a piece of spatial information concerning the disease and also the overlaps of different portions of the body may hide infected tissues. Additionally, several X-rays are complicated to review when lesions are in low contrast or overlap in large pneumonic veins. Sometimes, an expert radiologist also takes more time to read and address each X-ray image, which can cause misdiagnosis due to exhaustion. The field of clinical diagnosis quickly improves with the introduction of Artificial Intelligence and Machine Learning. With the development of computer technology and statistical Machine Learning algorithms, Computer-Aided Diagnosis (CAD) has achieved rapid growth in the field of medical imaging. CAD can overcome the problem of radiologists, including the discovery of small lesions, the analysis of morphology and lesions [19]. However, traditional computer vision mainly used various operators to extract the features of images and then classifies them by Machine Learning algorithms. The modern Machine Learning approach, called Deep Convolutional Neural Network (CNN), can abstract the high-dimensional expression of the image through convolution, downsampling, to effectively diagnose images. Since CNN is an end to end network and can be trained very easily, therefore it is very useful for diagnosing X-ray images. CNN does not require any expert for feature extraction as they are trained by using raw images and labeled data for classification. In recent years, several images based CAD systems are developed in the medical field [20,21,22,23,24,25]. Also, in another research work [26] Deep CNN model has been implemented successfully on a CXR dataset to classify pneumonia, which further motivates the use of Deep CNN for different image datasets.

In this work, a total of 2905 CXR images is used with 209 confirmed positive COVID-19 and 1341 positive pneumonia cases to train the CNN model for classifying them as novel COVID -19 diseases and normal images. To carry out this research, each X-ray image is labeled as a normal type or COVID-19 type or pneumonia type for CNN based automatic analysis. In the next step different CNN models are trained by using these labeled CXR images to find out three image classification problems: Classifying 1) COVID-19 images versus normal images (binary classification), 2) COVID-19 images versus pneumonia images (binary classification), 3) COVID-19 images versus pneumonia images versus normal images (multiclass classification problem). To perform this classification, two pre-trained CNN model of transfer learning VGG16 and InceptionV3 are used. Their performance is

finally compared using hyperparameter tuning and data augmentation techniques.

The remaining paper is structured as Section 2 explains the background of the methodology used in this paper. In section 3 and 4, the detailed experimental design and results are discussed. Finally, section 5 summarizes the conclusion and suggests further improvements in this direction.

## 2 Background

### 2.1 Convolutional Neural Network

A Convolutional Neural Network (CNN) is a class of feed-forward neural networks. CNN is built on top of four key ideas: local connection, sharing weights, pooling, and use of multiple layers. The architecture of a typical CNN (Figure 2) is composed of these layers; in a first part: convolution layer, ReLU (Rectified Linear Units), pooling layer and in a second part: fully connected layer, loss layer [27].

The convolution layer applies a set of discrete convolutions on the output of the previous layer. Each convolution is done using a kernel (also called: mask, filter bank) and produces a 2D feature map. This layer is also seen as a layer with local connections so that a neuron is connected only to neurons of the previous layer in the same region. Local connections give the ability to the layer to detect local patterns from the previous layer. Moreover, the weights of the local connections are shared among all neurons in the layer, this means that the same local pattern can be detected in the same way anywhere in the previous layer.

The ReLU applies a non-linear function  $f(x) = \max(0, x)$  to the output of the previous convolution layer. Other non-linear activation functions are available such as hyperbolic tangent, sigmoid function. The ReLU is the most common among these because the training of the neural network is faster using this function [28].

The pooling layer splits the output of the previous layer into a grid, then on each cell of the grid, a pooling function is applied and outputs only a single value. Thus, the pooling layer is a down-sampling step, the resolution of the grid can vary and affects the sampling

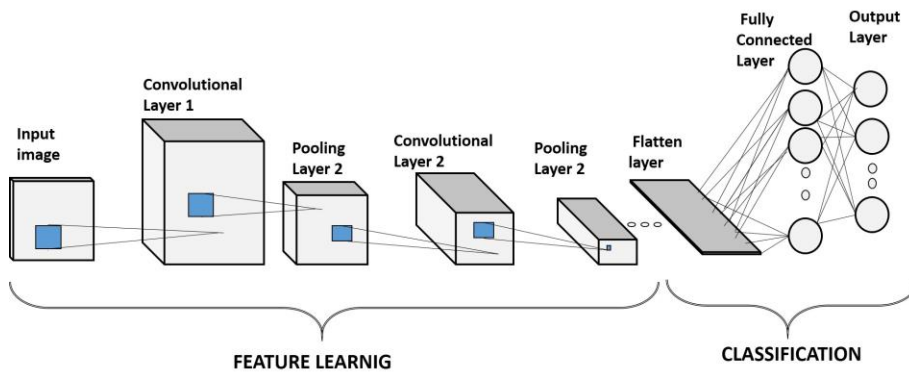


Fig. 2 Architecture of basic Convolutional Neural Network

rate. This layer merges multiple semantically similar features into one. Due to the down-sampling, the position of the feature is not accurately preserved, therefore an invariance to small shifts or distortions is spawned. The position of a feature is not as important as its relative position to other features. A typical pooling function outputs the maximum value of a local patch.

Repeating these layers several times in this order: convolution, ReLU, and pooling, one can exploit the fact that high-level features are composed of low-level features. The first group of layers can detect small details such as edges and contours. The second layer can detect higher-level features such as motifs. This process is repeated so that firstly, edges are merged into motifs, motifs into parts and finally parts into objects. The architecture of a very basic CNN is shown in Figure 2.

After the first part composed of convolution layers, ReLU, and pooling layers; a second part of the neural network is composed of fully-connected layers and a loss layer. Loss layers are used to train CNN using different functions such as softmax function and sigmoid cross entropy function. This second part is a classical feed-forward neural network used to classify the features coming from the first part. The training of CNN is possible using the backpropagation algorithm. Because of the local connectivity and the shared weights, there are lesser parameters in the model. Thus, the network is less prone to overfitting and gener-

alizes better. In addition to all these layers, the batch normalization and dropout techniques are also applied for improving the performance of CNN.

## 2.2 Image Classification Problem

Image classification is one of the biggest problems in the medical field. The major goal of medical image classification is to classify images of the different diseases setting possible labels. Using a deep learning approach this problem can be solved with the help of transfer learning. Transfer learning is one of the popular approaches in Machine Learning which can be useful for building an accurate and higher performance model in a short time-span. In computer science, transfer learning is expressed through the utilization of pre-trained model state-of-art CNN models. A pre-trained or previously trained model is a model trained on a large dataset to solve a problem close to the issue investigated in this paper.

In this paper, to solve the problem of chest x-ray classification and to improve the performance of a CNN model, two pre-trained CNN (VGG16 and InceptionV3) models for the ImageNet Large Scale Visual Recognition Challenge (ILSVRC) are presented. All of them are implemented in the Keras library and are used later in this paper.

### *The VGG16 Model*

The VGG network [29] was created in 2014 for ILSVRC. The authors investigated the effect of depth on accuracy. For that purpose, they use a simple convolutional neural network with very small (3x3) convolution filters with stride and pad of 1, 2x2 max-pooling with stride 2, and push the depth to 16-19 layers, which was sufficient at that time. To identify large images VGG16 models are used. This model is shown in Figure 3. VGG16 model was sent for the ILSVRC-2014 competition and trained for several weeks using NVIDIA TITAN BLACK video cards.

### *InceptionV3 Model*

The InceptionV3 network [31] was created in 2015. Instead of stacking convolutional and pooling layers sequentially on top of each other, some layers are in parallel and their results are merged periodically. As shown in Figure 4 from Google Research [32], the key idea of this network is to stack Inception modules, which are composed of convolutional and pooling layers. This can be easily seen in Figure 4. By using fewer weights than previous

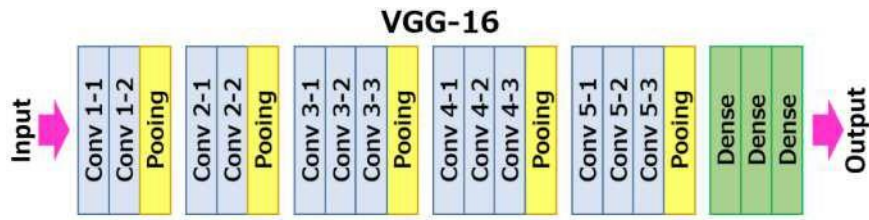


Fig. 3 VGG16 Model [30]

neural networks, for instance, about 30x fewer parameters than VGG19, the computational cost of InceptionV3 is suitable for big-data or mobile scenarios.

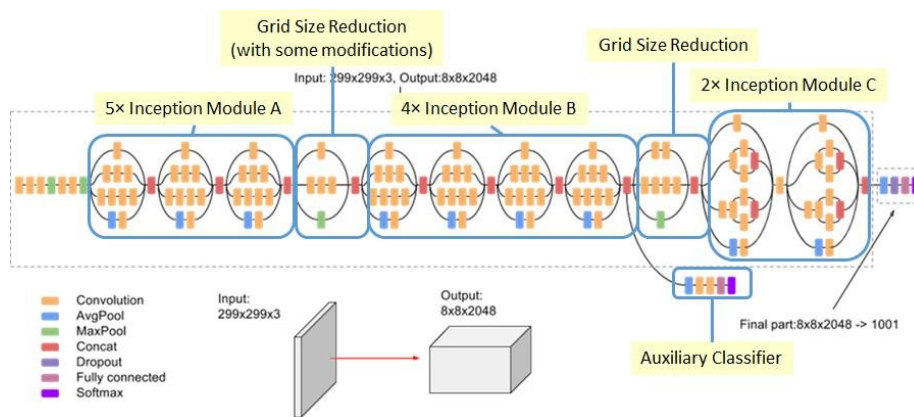


Fig. 4 Inception V3 Model [31]

### 3 Experimental Design

#### 3.1 Dataset

In this work, an online repository dataset [33] which is publicly available is used. It consists of three kinds of chest X-Ray images: Normal, Pneumonia and COVID-19, which are arranged in three directories. There are a total of 2905 images of chest X-rays with 1341 normal cases, 1345 positive pneumonia cases and 219 confirmed positive COVID-19. Figure 5 shows chest X-Rays from the Kaggle dataset. In the left panel of the figure chest x-ray

of a normal patient is given which depicts clear lungs as compared to the other two chest x-rays of pneumonia patient and COVID-19 patient.

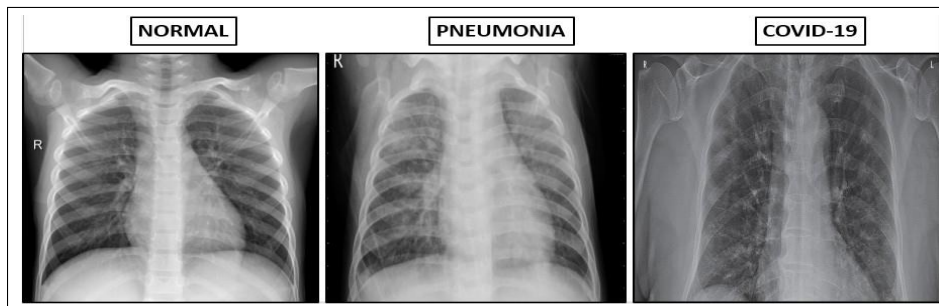


**Fig. 5** Examples of Chest X-Rays [33]

### 3.2 CNN Model Designs

The pre-trained CNN models are used to perform several types of classification by replacing its final layer neurons with an appropriate number of diseases. These models are used to perform three types of image classification problems: i) Classification of normal versus COVID-19 images, ii) Classification of COVID-19 versus Pneumonia images, and iii) Classifying normal versus COVID-19 versus Pneumonia images.

The process is started by using two pre-trained models, VGG16 and InceptionV3. The chest x-ray images are used as data input to train these models. The x-ray images are prepared at size 224 to 1024 for training the model using small computation.

### 3.3 Design of Data Augmentation and Fine-tuning

Data augmentation on image datasets can help to increase the number of relevant images in our database. This can help to increase the performance of pre-trained models. Therefore, to check the performance of our pre-trained models, three different ways of augmenting images are used as follows:

- Augmentation 0: This refers to the original image datasets without using any augmentation.

- Augmentation1: The simple geometrical transformation on images such as random flip, rotate, shear and zoom are performed to increase the original dataset by factor eighth.
- Augmentation1: Some complex geometrical transformation are performed to increase the original dataset by factor sixteen.

The database (2905 images only) used in this research work for this classification problem is too small as compared to the normal data required to train the pre-trained CNN models from ImageNet or GoogleNet, hence some layers are trained, keeping others frozen to fine-tune the model. In the CNN model, the layers at the bottom refer to features that are not depending upon the classification problem, whereas, layers at the top refers to the problem-dependent features. Also, there are very small numbers of images and large numbers of parameters, more layers are kept frozen. Hence, the choice is a very small model of pre-trained models with their last layer unfrozen. Both VGG16 and InceptionV3 model consist of two layers (group average pooling layer and softmax layer) after the convolution layer with a total number of 1026 and 4096 training parameters respectively and their last layer is made unfrozen. Then for training these models their hyperparameters are set as: *learning rate* = 0.05, *decay rate* = 0.9, *echo* = 40 and *batch.size* = 8.

*i. Classification Problem 1: Normal Vs COVID-19 Images*

In this classification problem, the data is labeled using two classes: normal (1341 images) and COVID-19 (209 images). This data is then split into 60% data for training, 10% data for validation, and 30% data for testing. The models are trained using this training dataset and then this trained model is used for classification of normal vs COVID-19 images using validation data.

*ii. Classification Problem 2: COVID-19 Vs Pneumonia Images*

This is also binary classification and hence similar to classification problem 1, again the data is labeled using two classes Pneumonia (1345 images) and COVID-19(209 images). The dataset is split by keeping 60% data for training, 10% data for validation, and 30% data for testing. The models are trained using this training data and then this trained model is used for classification of COVID-19 vs pneumonia images using validation data.

*iii. Classification Problem 3: Normal Vs COVID-19 Vs Pneumonia Images*

This is a multiclass classification problem and hence some modifications are required in the proposed network model. As the model is designed to predict three outputs (normal,

COVID-19 and Pneumonia), hence the last layer of the model is modified to three neurons. As done in the previous two problems, each training image is labeled by their appropriate disease label i.e., Normal Vs COVID-19 Vs Pneumonia. The biggest challenge here is the unbalanced data (Normal images-46.29% Vs COVID-19- 7.19 % Vs Pneumonia(46.16%). Hence, for data balancing, data augmentation is performed as discussed earlier.

#### 4 Result and Discussion

The experiments have been performed using the Python Jupyter notebook in Keras. For training the CNN model, a virtual machine in Google Cloud GPU with 32 GB of RAM and NVIDIA Tesla K80 is used. All the evaluations are carried out on a 30% dataset of all images. The results of all experiments are presented in this section.

##### 4.1 Performance Metrics

A confusion matrix is used to check how well a model can perform for new data. It is represented by using four values TP (True Positive), TN (True Negative), FP (False Positive), and FN (False Negative). In addition to this, accuracy, sensitivity, specificity, precision, recall and f1-score metric for detection are used. These are the commonly used metrics for measurement of model performance in medical research. f1-score is also a better metric to measure the success of the model's prediction. It is considered as the balance between precision and recall. Following equations (1) to (6) shows the formulae for different performance metric to measure the performance of binary classification models.

$$Accuracy = \frac{TP + TN}{TP + FP + TN + FN} \cdot 100 \quad (1)$$

$$sensitivity = \frac{TP}{TP + FN} \cdot 100 \quad (2)$$

$$speci ficity = \frac{TN}{TN + FP} \cdot 100 \quad (3)$$

$$Precision = \frac{TP}{TP + FP} \quad (4)$$

$$Recall = \frac{TP}{TP + FN} \quad (5)$$

$$f1 score = 2 \cdot \frac{Precision \cdot Recall}{Precision + Recall} \quad (6)$$

To measure the performance of multiclass classification models, the following equations (7) to (12) of performance measures are used.  $Acc_m$ ,  $sens_m$ ,  $spec_m$ ,  $Prec_m$ ,  $Recall_m$ ,  $f1\_score_m$  represents accuracy, sensitivity, specificity, precision, recall and f1-score metric of multiclass classification models respectively.

$$Acc_m = \frac{TP_n + TP_c + TP_p}{total\ samples} \cdot 100 \quad (7)$$

$$sens_m = \frac{TP_c + TP_p}{TP_c + TP_p + FN_c + FN_p} \cdot 100 \quad (8)$$

$$spec_m = \frac{TP_n}{FP_c + TP_n + FP_p} \cdot 100 \quad (9)$$

$$Prec_m = \frac{TP_c + TP_p}{TP_c + FP_c + TP_p + FP_p} \quad (10)$$

$$Recall_m = \frac{TP_c + TP_p}{TP_c + TP_p + FN_c + FN_p} \quad (11)$$

$$f1\_score_m = 2 \frac{Prec_m \cdot Recall_m}{Prec_m + Recall_m} \quad (12)$$

where,  $TP_c$  means COVID-19 positive patients predicted to be COVID-19 positive,  $TP_p$  means pneumonia positive patients predicted to be pneumonia positive,  $TP_n$  means normal patients predicted to be normal.  $FP_c$  normal penitents predicted to be COVID-19 positive,  $FP_p$  normal penitents predicted to be pneumonia positive,  $FN_c$  COVID-19 penitents predicted to be normal,  $FN_p$  pneumonia positive penitents predicted to be normal penitents.

#### 4.2 Results of Normal vs COVID-19 Classification and COVID-19 vs Pneumonia Images

The performance of both pre-trained models is evaluated. The highest accuracy is obtained for the InceptionV3 model for augmentation1 techniques in both the classifications. The training and testing times for these models are 1240 seconds and 10 seconds respectively for classification problem 1; whereas for the second classification problem, it is 1254 sec and 8 seconds respectively. Table 1 gives the comparison of three augmentation techniques and performance of both models on three augmentation techniques. It can be examined from the table, the results of the model improve with the increasing training images, and training with a large number of images can also affect the result of accuracy. However, the results can be further improved with large training data and fine-tuning of hyperparameters such as dropout rate, learning rate, batch normalization layers.

**Table 1** Classification report of : A) COVID-19 vs Normal models, and B) COVID-19 Vs Pneumonia

| A. Normal Vs COVID-19    |                        |                 |              |              |              |              |              |              |
|--------------------------|------------------------|-----------------|--------------|--------------|--------------|--------------|--------------|--------------|
| Model                    | Augmentation Technique | Training Images | Accuracy     | Sensitivity  | Specificity  | Precision    | Recall       | f1-score     |
| VGG16                    | augmentation0          | 2905            | 91.66        | 94.66        | 85.89        | 0.928        | 0.946        | 0.937        |
|                          | augmentation1          | 15000           | 97.71        | 98.53        | 96.15        | 0.9801       | 0.985        | 0.982        |
|                          | augmentation2          | 30000           | 93.85        | 98.66        | 84.61        | 0.925        | 0.986        | 0.954        |
| InceptionV3              | augmentation0          | 2905            | 95.61        | 97.33        | 92.30        | 0.96         | 0.973        | 0.966        |
|                          | <b>augmentation1</b>   | <b>15000</b>    | <b>99.35</b> | <b>99.50</b> | <b>98.41</b> | <b>0.997</b> | <b>0.995</b> | <b>0.996</b> |
|                          | augmentation2          | 30000           | 97.01        | 98.66        | 93.84        | 0.968        | 0.986        | 0.977        |
| B. COVID-19 Vs Pneumonia |                        |                 |              |              |              |              |              |              |
| Model                    | Augmentation Technique | Training Images | Accuracy     | Sensitivity  | Specificity  | Precision    | Recall       | f1-score     |
| VGG16                    | augmentation0          | 2905            | 90.08        | 94.4         | 81.79        | 0.908        | 0.944        | 0.926        |
|                          | augmentation1          | 15000           | 96.27        | 97.33        | 92.02        | 0.95         | 0.973        | 0.963        |
|                          | augmentation2          | 30000           | 93.59        | 96.26        | 88.46        | 0.941        | 0.962        | 0.951        |
| InceptionV3              | augmentation0          | 2905            | 94.64        | 98.53        | 87.17        | 0.936        | 0.985        | 0.96         |
|                          | <b>augmentation1</b>   | <b>15000</b>    | <b>98.29</b> | <b>98.27</b> | <b>98.41</b> | <b>0.99</b>  | <b>0.982</b> | <b>0.99</b>  |
|                          | augmentation2          | 30000           | 96.40        | 98.66        | 92.05        | 0.959        | 0.986        | 0.973        |

The left part of Figure 6 shows the confusion matrix for best model InceptionV3 in classification problem 1 i.e., Normal vs COVID-19. It can be seen that the number of normal patients predicted to be positive COVID-19 (false negative) is 2 means it has very high sensitivity and also the number of COVID-19 patients predicted as normal is very small i.e. 1 means it has very high specificity.

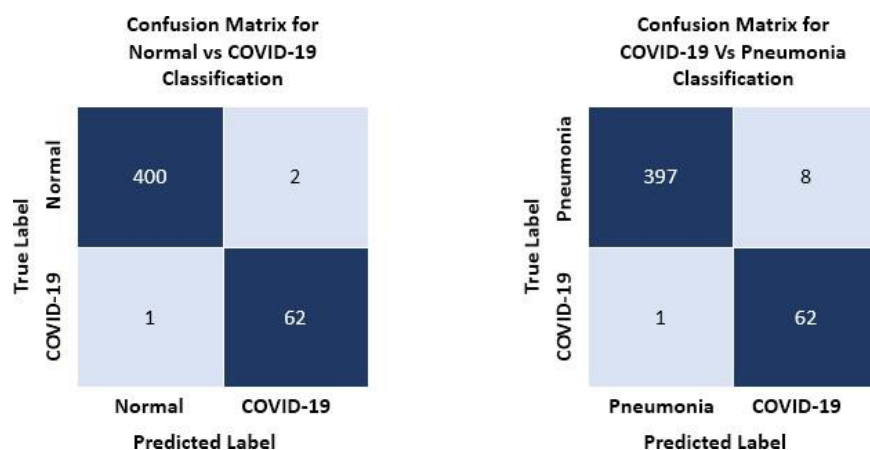


**Fig. 6** Confusion matrices for classification problem a and 2 for best model InceptionV3

Similarly, the right part of Figure 6 shows the confusion matrix for best model InceptionV3 in classification problem 2 i.e., Pneumonia vs COVID-19. Further from this matrix, it can be concluded that the model has high sensitivity and specificity. In addition to this, if f-1 score of both the models is calculated using precision and recall metric, then it is almost 1 for both the models. A very high F1-score indicates that the model can predict disease with a 99.5% success rate.

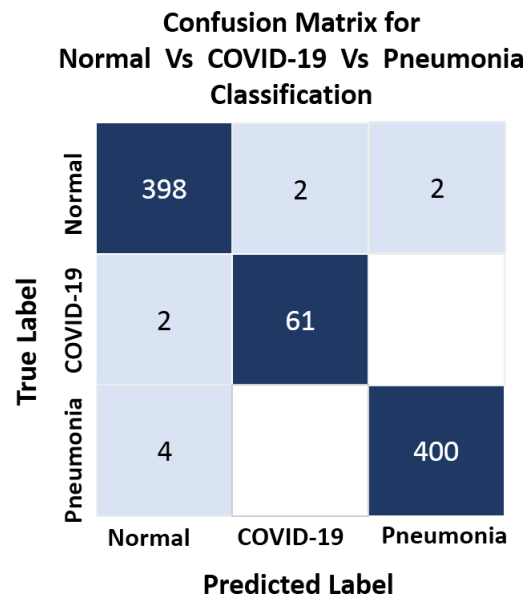
#### 4.3 Results of Normal vs COVID-19 vs Pneumonia Classification

Table 2 shows the model performance of each label, it is seen that models perform well for a large number of image data here as well. In this case, the VGG16 model performs better than InceptionV3. The model InceptionV3 in all cases i.e. the model is recognizing the correct disease in all three labels (Normal, COVID-19 and Pneumonia), reaching almost 99% accuracy. As a computer-aided diagnosing system these three labels are very much important for the classification of these labels. However, when the training images are very small or very large in numbers, neither models predict better results. The reason behind this is i) Since for small dataset the proposed models maybe under-fitted due to large number parameters in the pre-trained network used in these models for transfer learning, and ii) As data augmentations are used for creating a large dataset that consists of complex and

large transformation which can add a certain amount of noise to the training set which may influence the training process. These two reasons may reduce the performance of our models.

**Table 2** Classification report of Normal vs COVID-19 Vs Pneumonia

| Model       | Augmentation Technique | Training Images | $Acc_m$      | $sens_m$     | $spec_m$     | $Prec_m$     | $Recall_m$   | $f1-score_m$ |
|-------------|------------------------|-----------------|--------------|--------------|--------------|--------------|--------------|--------------|
| VGG16       | augmentation0          | 2905            | 96.66        | 98.13        | 93.84        | 0.96         | 0.981        | 0.974        |
|             | <b>augmentation1</b>   | <b>15000</b>    | <b>98.84</b> | <b>98.71</b> | <b>99.00</b> | <b>0.991</b> | <b>0.987</b> | <b>0.988</b> |
|             | augmentation2          | 30000           | 97.36        | 98.66        | 94.87        | 0.973        | 0.986        | 0.98         |
| InceptionV3 | augmentation0          | 2905            | 93.85        | 96.66        | 88.46        | 0.941        | 0.966        | 0.953        |
|             | augmentation1          | 15000           | 96.35        | 96.66        | 92.82        | 0.962        | 0.966        | 0.964        |
|             | augmentation2          | 30000           | 93.77        | 95.86        | 89.74        | 0.947        | 0.958        | 0.952        |



**Fig. 7** Confusion matrices for classification problem 2 for best model VGG16

The confusion matrix for best model VGG16 in classification problem 2 (Normal Vs COVID-19 Vs Pneumonia) is shown in Figure 7. It can be seen that the number of correct predictions ( $TP_n$ ,  $TP_c$ , and  $TP_p$ ) are very high as compared to wrong predictions ( $FP_c$ ,  $FP_p$ ,  $FN_p$ , and  $FN_c$ )

which are very small in number. Therefore, it is concluded that the proposed model has very high f1-score.

## 5 Conclusion

In this paper, the COVID-19 images, Normal and Pneumonia X-Ray images are classified using the CNN model. The experiments are carried out keeping in mind the computer science perspective. It is concluded that for binary classification InceptionV3 performed better than the VGG16 model. Whereas, for multiclass classification VGG16 outperformed InceptionV3. The results also show that augmentation is helpful in a small database. However, it is also been found that augmenting a large number of images from a small set of images influences model accuracy because of the addition of noise during model training. On the other hand, a very small number of images did not produce the best result for any model due to the underfitting problems in the pre-trained model. The dataset is downloaded from an open-source online repository. The promising results obtained using CNN models suggest that Chest X-Ray can be useful for early detection of the Coronavirus as compared to the time-consuming pathological test or costly CT-Scan. The study consists of very small data images for model training, so it will be interesting to see the effect of large data and the use of other pre-trained models in future work.

## Compliance with Ethical Standards

### Funding

No funding was received for this study.

### Conflict of interest

The authors declare no conflict of interest, financial or otherwise.

### Research involving human participants and/or animals

This research paper does not contain any studies with human participants or animals performed by any of the authors.

## Ethical approval

Not needed.

## Informed consent

All authors agreed on the submitted version.

## References

1. D. Thomas-Rüddel, J. Winning, P. Dickmann, D. Ouart, A. Kortgen, U. Janssens, and M. Bauer, "Coronavirus disease 2019 (covid-19): update for anesthesiologists and intensivists march 2020," *Der Anaesthetist*, pp. 1–10, 2020.
2. N. Zhu, D. Zhang, W. Wang, X. Li, B. Yang, J. Song, X. Zhao, B. Huang, W. Shi, R. Lu *et al.*, "A novel coronavirus from patients with pneumonia in china, 2019," *New England Journal of Medicine*, 2020.
3. Q. Li, X. Guan, P. Wu, X. Wang, L. Zhou, Y. Tong, R. Ren, K. S. Leung, E. H. Lau, J. Y. Wong *et al.*, "Early transmission dynamics in wuhan, china, of novel coronavirus–infected pneumonia," *New England Journal of Medicine*, 2020.
4. "World health organization," <https://www.who.int/news-room/articles-detail/updated-who-recommendations-for-international-traffic-in-relation-to-covid-19-outbreak>, accessed: 2020-08-03.
5. "Covid-19 coronavirus pandemic," <https://www.worldometers.info/coronavirus/>, accessed: 2020-08-03.
6. C. Sohrabi, Z. Alsafi, N. O'Neill, M. Khan, A. Kerwan, A. Al-Jabir, C. Iosifidis, and R. Agha, "World health organization declares global emergency: A review of the 2019 novel coronavirus (covid-19)," *International Journal of Surgery*, 2020.
7. Y. Yang, Q. Lu, M. Liu, Y. Wang, A. Zhang, N. Jalali, N. Dean, I. Longini, M. E. Halloran, B. Xu *et al.*, "Epidemiological and clinical features of the 2019 novel coronavirus outbreak in china," *medRxiv*, 2020.
8. N. Chen, M. Zhou, X. Dong, J. Qu, F. Gong, Y. Han, Y. Qiu, J. Wang, Y. Liu, Y. Wei *et al.*, "Epidemiological and clinical characteristics of 99 cases of 2019 novel coronavirus pneumonia in wuhan, china: a descriptive study," *The Lancet*, vol. 395, no. 10223, pp. 507–513, 2020.
9. C. Huang, Y. Wang, X. Li, L. Ren, J. Zhao, Y. Hu, L. Zhang, G. Fan, J. Xu, X. Gu *et al.*, "Clinical features of patients infected with 2019 novel coronavirus in wuhan, china," *The Lancet*, vol. 395, no. 10223, pp. 497–506, 2020.
10. D. K. Chu, Y. Pan, S. M. Cheng, K. P. Hui, P. Krishnan, Y. Liu, D. Y. Ng, C. K. Wan, P. Yang, Q. Wang *et al.*, "Molecular diagnosis of a novel coronavirus (2019-ncov) causing an outbreak of pneumonia," *Clinical chemistry*, vol. 66, no. 4, pp. 549–555, 2020.
11. T. Ai, Z. Yang, H. Hou, C. Zhan, C. Chen, W. Lv, Q. Tao, Z. Sun, and L. Xia, "Correlation of chest ct and rt-pcr testing in coronavirus disease 2019 (covid-19) in china: a report of 1014 cases," *Radiology*, p. 200642, 2020.

12. S. Wang, B. Kang, J. Ma, X. Zeng, M. Xiao, J. Guo, M. Cai, J. Yang, Y. Li, X. Meng *et al.*, "A deep learning algorithm using ct images to screen for corona virus disease (covid-19)," *medRxiv*, 2020.
13. V. M. Corman, O. Landt, M. Kaiser, R. Molenkamp, A. Meijer, D. K. Chu, T. Bleicker, S. Brünink, J. Schneider, M. L. Schmidt *et al.*, "Detection of 2019 novel coronavirus (2019-ncov) by real-time rt-pcr," *Eurosurveillance*, vol. 25, no. 3, p. 2000045, 2020.
14. M.-Y. Ng, E. Y. Lee, J. Yang, F. Yang, X. Li, H. Wang, M. M.-s. Lui, C. S.-Y. Lo, B. Leung, P.-L. Khong *et al.*, "Imaging profile of the covid-19 infection: radiologic findings and literature review," *Radiology: Cardiothoracic Imaging*, vol. 2, no. 1, p. e200034, 2020.
15. J. P. Kanne, B. P. Little, J. H. Chung, B. M. Elicker, and L. H. Ketai, "Essentials for radiologists on covid-19: an updaterradiology scientific expert panel," 2020.
16. H. L. Fred, "Drawbacks and limitations of computed tomography: views from a medical educator," *Texas Heart Institute Journal*, vol. 31, no. 4, p. 345, 2004.
17. A. S. Bhalla, A. Goyal, R. Guleria, and A. K. Gupta, "Chest tuberculosis: Radiological review and imaging recommendations," *The Indian journal of radiology & imaging*, vol. 25, no. 3, p. 213, 2015.
18. P. S. Ngoya, W. E. Muhogora, and R. D. Pitcher, "Defining the diagnostic divide: an analysis of registered radiological equipment resources in a low-income african country," *The Pan African medical journal*, vol. 25, 2016.
19. C. Qin, D. Yao, Y. Shi, and Z. Song, "Computer-aided detection in chest radiography based on artificial intelligence: a survey," *Biomedical engineering online*, vol. 17, no. 1, p. 113, 2018.
20. L. Shen, L. R. Margolies, J. H. Rothstein, E. Fluder, R. McBride, and W. Sieh, "Deep learning to improve breast cancer detection on screening mammography," *Scientific reports*, vol. 9, no. 1, pp. 1–12, 2019.
21. Y. Dong, Z. Jiang, H. Shen, W. D. Pan, L. A. Williams, V. V. Reddy, W. H. Benjamin, and A. W. Bryan, "Evaluations of deep convolutional neural networks for automatic identification of malaria infected cells," in *2017 IEEE EMBS International Conference on Biomedical & Health Informatics (BHI)*. IEEE, 2017, pp. 101–104.
22. S. Khan and S.-P. Yong, "A deep learning architecture for classifying medical images of anatomy object," in *2017 Asia-Pacific Signal and Information Processing Association Annual Summit and Conference (APSIPA ASC)*. IEEE, 2017, pp. 1661–1668.
23. P. Gómez, M. Semmler, A. Schützenberger, C. Bohr, and M. Döllinger, "Low-light image enhancement of high-speed endoscopic videos using a convolutional neural network," *Medical & biological engineering & computing*, vol. 57, no. 7, pp. 1451–1463, 2019.
24. J. Choe, S. M. Lee, K.-H. Do, G. Lee, J.-G. Lee, S. M. Lee, and J. B. Seo, "Deep learning-based image conversion of ct reconstruction kernels improves radiomics reproducibility for pulmonary nodules or masses," *Radiology*, vol. 292, no. 2, pp. 365–373, 2019.
25. F. Shan+, Y. Gao+, J. Wang, W. Shi, N. Shi, M. Han, Z. Xue, D. Shen, and Y. Shi, "Lung infection quantification of covid-19 in ct images with deep learning," *arXiv preprint arXiv:2003.04655*, 2020.
26. S. S. Yadav and S. M. Jadhav, "Deep convolutional neural network based medical image classification for disease diagnosis," *Journal of Big Data*, vol. 6, no. 1, p. 113, 2019.
27. F. Tu, S. Yin, P. Ouyang, S. Tang, L. Liu, and S. Wei, "Deep convolutional neural network architecture with reconfigurable computation patterns," *IEEE Transactions on Very Large Scale Integration (VLSI) Systems*, vol. 25, no. 8, pp. 2220–2233, 2017.

28. A. Krizhevsky, I. Sutskever, and G. E. Hinton, "Imagenet classification with deep convolutional neural networks," in *Advances in neural information processing systems*, 2012, pp. 1097–1105.
29. K. Simonyan and A. Zisserman, "Very deep convolutional networks for large-scale image recognition," *arXiv preprint arXiv:1409.1556*, 2014.
30. M. ul Hassan, "Vgg16-convolutional network for classification and detection," *Neurohive. Dostopno na: https://neurohive.io/en/popular-networks/vgg16/[10. 4. 2019]*, 2018.
31. C. Szegedy, V. Vanhoucke, S. Ioffe, J. Shlens, and Z. Wojna, "Rethinking the inception architecture for computer vision," in *Proceedings of the IEEE conference on computer vision and pattern recognition*, 2016, pp. 2818–2826.
32. "Train your own image classifier," <https://research.googleblog.com/2016/03/train-your-own-image-classifier-with.html>, accessed: 2020-04-08.
33. "Covid-19 radiography database," <https://www.kaggle.com/tawsifurrahman/covid19-radiography-database>, accessed: 2020-04-08.

# Figures

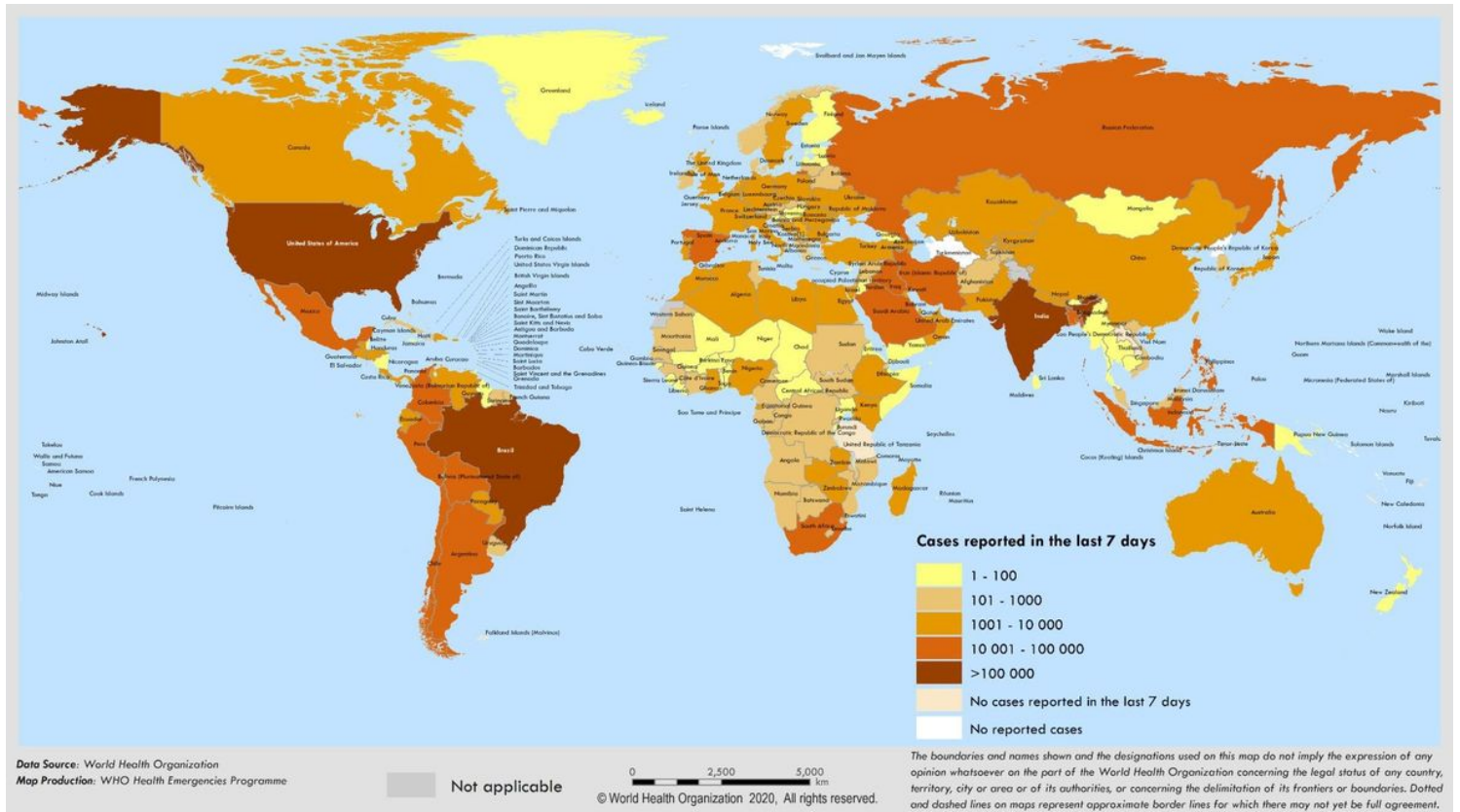


**Figure 1**

Total confirmed cases of COVID-19 by country and territory (as of 20 April 2020) [4]. Note: The designations employed and the presentation of the material on this map do not imply the expression of any opinion whatsoever on the part of Research Square concerning the legal status of any country, territory, city or area or of its authorities, or concerning the delimitation of its frontiers or boundaries. This map has been provided by the authors.

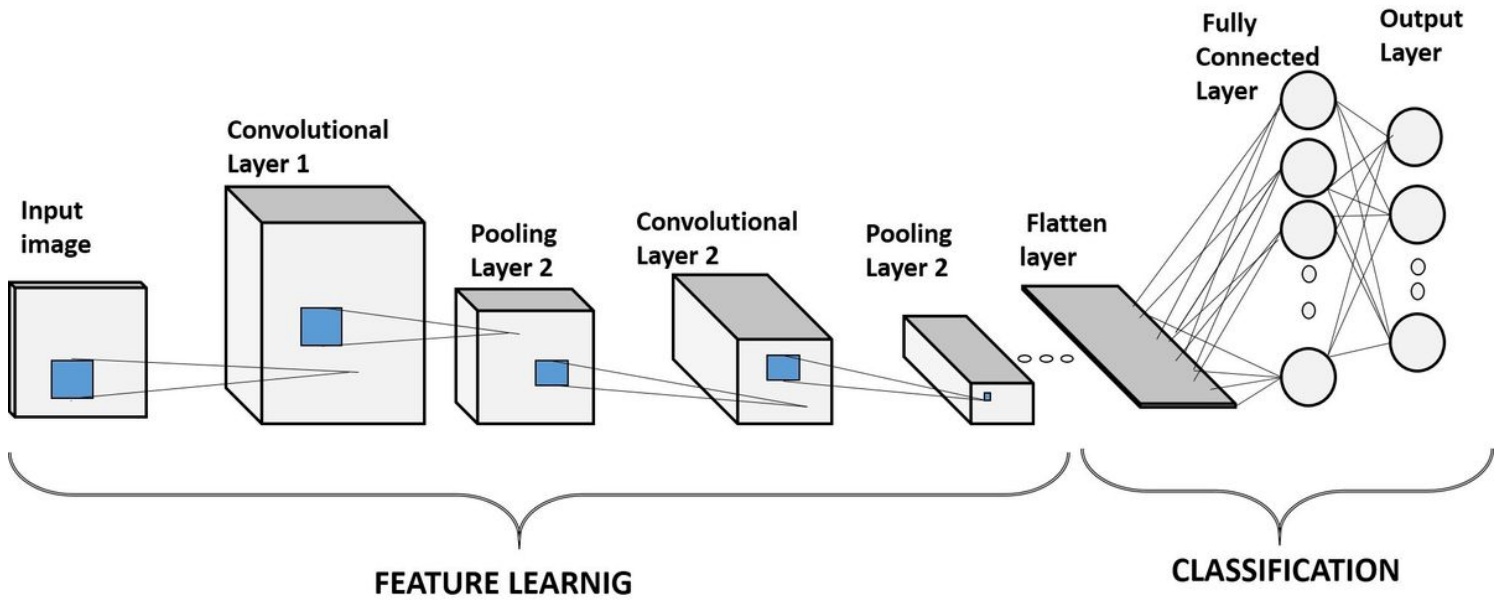


Figure 2

Architecture of basic Convolutional Neural Network

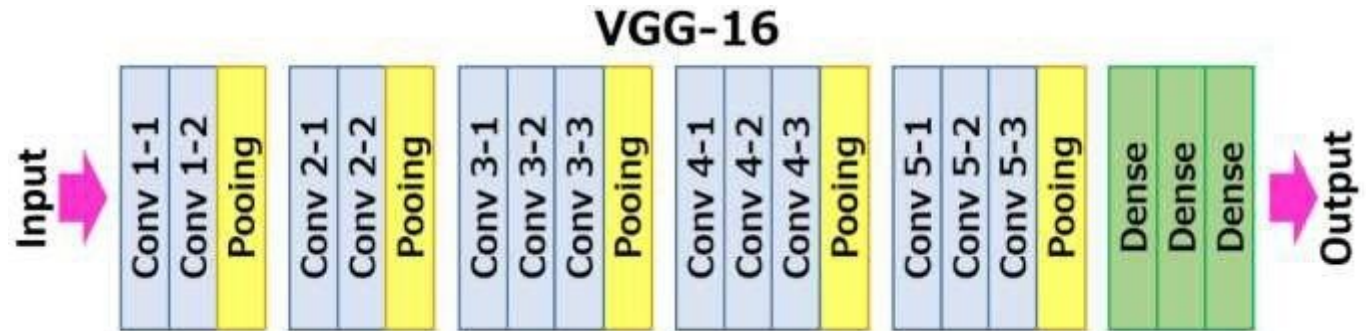


Figure 3

VGG16 Model [30]

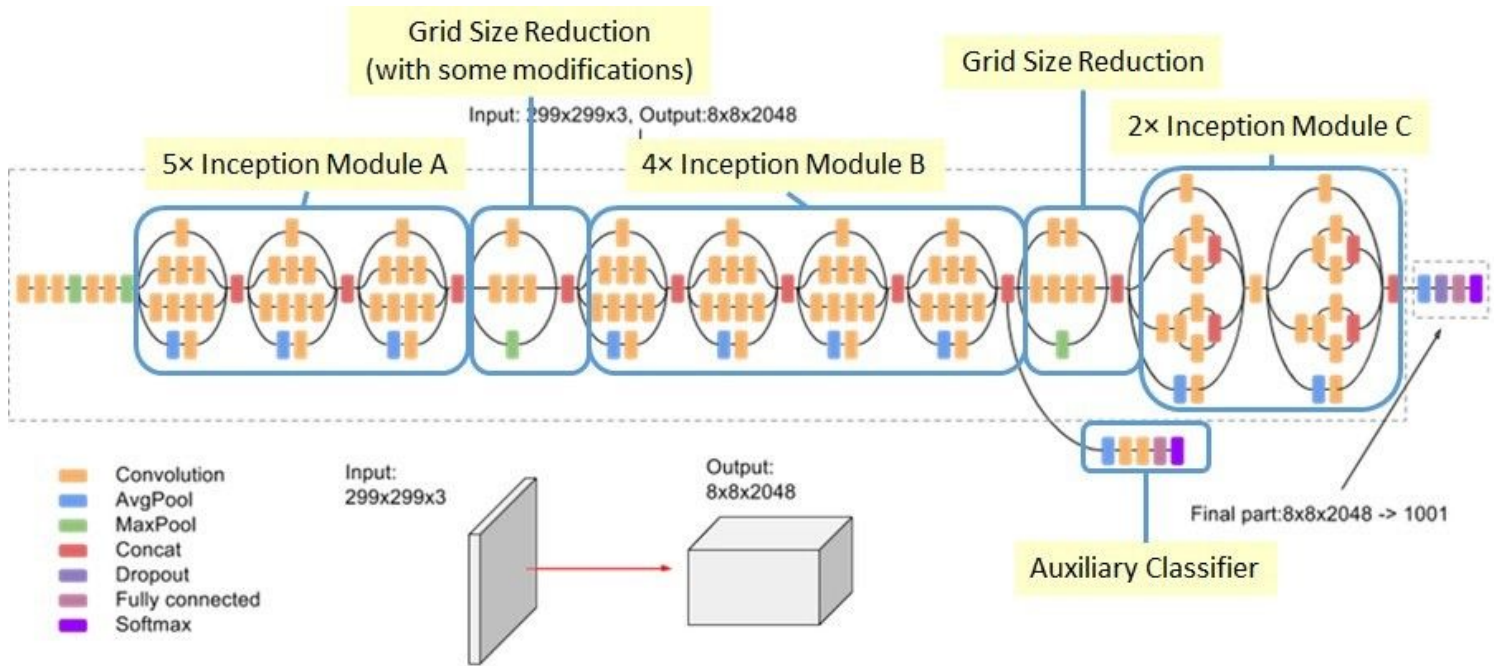


Figure 4

Inception V3 Model [31]

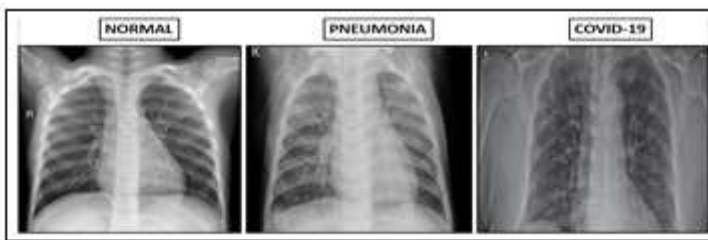


Figure 5

Examples of Chest X-Rays [33]

Confusion Matrix for Normal vs COVID-19 Classification

|            |          |                 |          |
|------------|----------|-----------------|----------|
| True Label | Normal   | 400             | 2        |
|            | COVID-19 | 1               | 62       |
|            |          | Normal          | COVID-19 |
|            |          | Predicted Label |          |

Confusion Matrix for COVID-19 Vs Pneumonia Classification

|            |           |                 |          |
|------------|-----------|-----------------|----------|
| True Label | Pneumonia | 397             | 8        |
|            | COVID-19  | 1               | 62       |
|            |           | Pneumonia       | COVID-19 |
|            |           | Predicted Label |          |

Figure 6

Confusion matrices for classification problem a and 2 for best model InceptionV3

## Confusion Matrix for Normal Vs COVID-19 Vs Pneumonia Classification

| True Label | Predicted Label |          |           |
|------------|-----------------|----------|-----------|
|            | Normal          | COVID-19 | Pneumonia |
| Normal     | 398             | 2        | 2         |
| COVID-19   | 2               | 61       | 0         |
| Pneumonia  | 4               | 0        | 400       |

Figure 7

Confusion matrices for classification problem 2 for best model VGG16